Biochemical and Biophysical Research Communications 483 (2017) 680–686

Contents lists available at ScienceDirect

Biochemical and Biophysical Research Communications

journal homepage: www.elsevier.com/locate/ybbrc

Distinct responses of compartmentalized glutathione redox potentials to pharmacologic quinones targeting NQO1

Vladimir L. Kolossov*, Nagendraprabhu Ponnuraj, Jessica N. Beaudoin, Matthew T. Leslie, Paul J. Kenis, H. Rex Gaskins

Carl R. Woese Institute for Genomic Biology, University of Illinois at Urbana-Champaign, Urbana, IL 61801, United States

ARTICLE INFO

Article history:
Received 7 December 2016
Accepted 12 December 2016
Available online 14 December 2016

Keywords:
Redox homeostasis
DNQ and β-lapachone
NQO1
Lung and pancreatic cancer
roGFP2 redox probe

ABSTRACT

Deoxynyboquinone (DNQ), a potent novel quinone-based antineoplastic agent, selectively kills solid cancers with overexpressed cytosolic NAD(P)H:quinone oxidoreductase-1 (NQO1) via excessive ROS production. A genetically encoded redox-sensitive probe was used to monitor intraorganellar glutathione redox potentials (E_{GSH}) as a direct indicator of cellular oxidative stress following chemotherapeutic administration. Beta-lapachone (β-lap) and DNQ-induced spatiotemporal redox responses were monitored in human lung A549 and pancreatic MIA-PaCa-2 adenocarcinoma cells incubated with or without dicumarol and ES936, potent NQO1 inhibitors. Immediate oxidation of E_{GSH} in both the cytosol and mitochondrial matrix was observed in response to DNQ and β-lap. The DNQ-induced cytosolic oxidation was fully prevented with NQO1 inhibition, whereas mitochondrial oxidation in A549 was NQO1-independent in contrast to MIA-PaCa-2 cells. However, at pharmacologic concentrations of β-lap both quinone-based substrates directly oxidized the redox probe, a possible sign of off-target reactivity with cellular thiols. Together, these data provide new evidence that DNQ's direct and discerning NQO1 substrate specificity underlies its pharmacologic potency, while β-lap elicits off-target responses at its effective doses.

1. Introduction

Current chemotherapeutic strategies for challenging solid tumors attempt to target cancer-specific processes in order to spare normal cells from damage. Disrupting redox homeostasis in ROS-burdened cancer cells is a proven anticancer strategy [1]. In normal cells, a phase II flavoenzyme NAD(P)H:quinone oxidoreductase-1 (NQO1, EC 1.6.99.2) is inducibly expressed to detoxify potentially mutagenic and carcinogenic quinones [2,3]. NQO1 catalyzes a two-electron reduction of various quinones to hydroquinones which can then be readily conjugated with glutathione or glucuronic acid and excreted from cells. However, certain quinones redirect NQO1 to a “futile redox cycle” where unstable hydroquinone spontaneously re-oxidizes to parental compounds, resulting in drastically elevated levels of superoxide anion which is subsequently metabolized by superoxide dismutase into hydrogen peroxide, thereby causing cellular oxidative damage [2,3]. Since NQO1 is highly up-regulated in the cytosol of most solid tumors, particularly in non–small cell lung, prostate, pancreatic, and breast cancers, this enzyme is an attractive chemotherapeutic target [4,5].

The quinone derived chemotherapeutic drug 1,2-naphthoquinone (aka β-lapachone), produced by the Lapacho tree, was reported to selectively kill NQO1-upregulated solid cancers *in vitro* and *in vivo* [2,4,5]. B-lapachone (β-lap, clinical ARQ 761) has shown great promise in medical trials, but more potent tumor-selective compounds with decreased off-target side effects are needed [6]. Recently, side-by-side comparison of the efficacy of various NQO1 quinone-based substrates in their ability to kill cancer cells in culture in an NQO1-dependent manner showed that deoxynyboquinone (DNQ) has a 10-fold superior efficacy to β-lap [7–9].

Early reports focused on the cytosolic activity of NQO1 as a principal determinant of β-lap and DNQ cytotoxicity, whereas the role of mitochondria is less understood. Both mitochondrial and NQO1 activities were reported in β-lap bioreduction in mouse melanoma B16–F10 cells expressing low NQO1 activity [10]. The data indicated the mitochondrial electron transport chain, specifically respiratory complex I, to be a principal factor in redox activation of β-lap [10]. Although the main mechanism of cancer cell

* Corresponding author.
E-mail address: viadimer@illinois.edu (V.L. Kolossov).

http://dx.doi.org/10.1016/j.bbrc.2016.12.082
0006-291X/

killing by β-lap is ROS-dependent, recent evidence suggested an alternative, ROS-independent, pathway for β-lap toxicity [11]. These results imply that chemotherapeutic quinones may react with multiple cellular constituents to promote cancer cell death, and the efficacy of NQO1-bioactivatable drugs may be improved by concomitant targeting of several cancer-specific metabolic pathways [6,12]. Together, these findings open a great potential in expanding antitumor therapeutic windows of NQO1-targeting drugs.

The cytotoxicity exerted by β-lap and DNQ is determined by both their dosage and the activity of intracellular antioxidant enzymes [6,13,14]. Furthermore, DNQ upregulates glutathione-specific genes, both catalytic and regulatory subunits of glutamate-cysteine ligase, in breast cancer cells [15]. Therefore, we reasoned that the formation of ROS resulting from the bioactivation of quinone substrates would be mediated by the glutathione system, the major antioxidant in mammalian cells [16,17]. Recent synthesis of DNQ analogues using computationally guided design and subsequent live-dead assays confirmed that DNQ is an exceptional NQO1 substrate that induces DNA damage, hyperactivates PARP1, causes dramatic losses of NAD^+ and ATP, and finally results in energy depletion and programmed necrosis [9]. However, whether NQO1 enzymatic activity is the only determinant causing DNQ-mediated ROS generation in both cytosol and mitochondria of NQO1-enriched cancer cells is unknown.

The aim of the present study was to define the real-time changes in subcellular glutathione redox homeostasis arising from DNQ-induced ROS production in NQO1-enriched human lung and pancreatic cancer cells. A genetically encoded fluorescent probe, enabling real-time monitoring of the drug-induced changes in compartmentalized glutathione redox potentials (E_{GSH}), and inhibitors of NQO1 enzymatic activity were foundational to the study [18,19]. We provide evidence indicating that increased cytosolic oxidation by DNQ relative to β-lap is a result of its outstanding NQO1 substrate specificity in NQO1-enriched cancer cells, while mitochondrial oxidative responses to DNQ are cell type dependent.

2. Materials and methods

2.1. Materials

Unless stated otherwise, reagents were obtained from Sigma (St. Louis, MO, USA). Lipofectamine 2000 was purchased from Invitrogen (Carlsbad, CA, USA). DNQ and its derivatives were kind gifts of Dr. Paul Hergenrother (University of Illinois, IL, USA). MitoSOX Red and the cationic dye tetramethylrhodamine ethyl ester (TMRE) were purchased from Life Technologies (Grand Island, NY, USA). All quinones were dissolved in dimethyl sulfoxide (DMSO).

2.2. Genetic constructs

The cytosolic and mitochondrial redox-sensitive sensors Grx1-roGFP2 were cloned into lentiviral pCDH-CMV-MCS-EF1-puro vector (System Biosciences, CA, USA). To target the probe to mitochondria, the mitochondrial matrix targeting sequence adenosine triphosphate synthase protein 9 originating from the fungus *Neurospora crassa* was used [20]. Grx1-roGFP2 in pQE60 and mito-Grx1-roGFP2 in pLPCX were kind gifts from Dr. Tobias Dick (Cancer Research Center, Heidelberg, Germany).

2.3. Cell culture, transfection, and cell sorting

A549 and MIA-PaCa-2 cells were provided by Dr. Hergenrother (University of Illinois, IL, USA). CHO cells were obtained from ATCC (Manassas, VA, USA). Cells were cultured at 37 °C with 5% CO_2 in RPMI 1640 (A549) or DMEM (CHO, MIA-PaCa-2) media supplemented with 10% FBS (University of Illinois Cell Media Facility, Urbana, IL, USA). Lentiviral transfection using lipofectamine was performed as suggested by manufacturer, and fluorescence activated cell sorting was described elsewhere [21].

2.4. Measurement of mitochondrial ROS levels by confocal microscopy

MitoSOX Red dye was used to analyze the extent of ROS generation by mitochondria via confocal microscopy as described previously [22].

2.5. Measurement of mitochondrial transmembrane potential

Time-dependent changes in mitochondrial transmembrane potential were measured using the cationic dye TMRE. To assess alteration in mitochondrial membrane potential, cells in Dulbecco's phosphate-buffered saline supplemented with 5% FBS and 10 mM glucose were exposed to 50 nM TMRE and incubated with 0.6 μM DNQ for various times. Data were acquired every 10 min using a BD LSR II (Becton Dickson, San Jose, CA) flow cytometer, with at least 10,000 cells per sample. The 488 nm laser line at 20 mW was used to excite TMRE dye. Fluorescence was collected using 575/26 nm bandpass filter along with 550 nm long-pass dichroic splitter. The data were analyzed using FACS Express Version 3 (De Novo Software, Thornhill, Ontario, Canada).

2.6. Live cell imaging and image processing

Image acquisition of live cells stably transfected with cytosolic or mitochondrial Grx1-roGFP2 probe was performed in μ-Slide eight-well ibiTreat microscopy chambers (Ibidi, Munich, Germany). The cells were washed twice with Dulbecco's phosphate-buffered saline supplemented with 5% FBS and 10 mM glucose prior to imaging. Time-lapse images were collected with a fluorescence-enabled inverted microscope (Axiovert 200 M, Carl Zeiss, Feldbach, Switzerland) using an imaging protocol discussed in detail elsewhere [20]. Time-resolved images were acquired every 15 s or 30 s at a 512 × 512 pixel resolution. The region of interest (ROI) used for analysis was always a well-defined cytosolic or mitochondrial compartment. Images were exported to the Axiovision software in which ROI intensities were calculated and the background fluorescence intensity was subtracted. All results were analyzed by ANOVA, and are expressed as mean ± SD [20].

3. Results and discussion

3.1. Cytosol and mitochondria respond distinctly to NQO1-bioactivable quinone DNQ

The role of cytosolic NQO1 in quinone-based cytotoxicity is characterized by induction of extensive ROS generation which leads to tumor-selective killing [4,5,23]. Human lung A549 and pancreatic ductal MIA-PaCa-2 adenocarcinoma cell lines with well-characterized levels of NQO1 activity, 2700 nmol/min/μg and 1130 nmol/min/μg, respectively, were selected as cancer cell models of oxidative stress following chemotherapeutic administration [9]. Green fluorescent protein-based redox biosensors enable real-time monitoring of compartmentalized glutathione redox potentials in live cells [19]. Specifically we have utilized the Grx1-roGFP2 biosensor, which features a glutaredoxin 1 (Grx1) enzyme fused to the cysteine-based roGFP2 biosensor, thereby improving its specificity and response kinetics to alterations in glutathione redox potentials [18]. To monitor DNQ-induced

oxidative responses in the cytosol and mitochondrial matrix in real-time, the redox-sensitive cytoGrx1-roGFP2 (cGFP2) and mitoGrx1-roGFP2 (mGFP2) sensors were expressed in the respective compartments of NQO1-expressing A549 and MIA-PaCa-2 cells [4].

Fig. 1 shows fluorescence images of A549 and MIA-PaCa-2 cells expressing the redox probes in cytosol and mitochondria with the corresponding ratiometric analysis depicted below following exposure to DNQ in the absence or presence of dicumarol and ES936, potent inhibitors of NQO1. The mitochondrial probe exhibits the characteristic tubular shape of the organelle, while in the cytosol fluorescence is diffusely distributed [20]. Ratiometric analysis of time course imaging is expressed through the time resolved changes in excitation ratio of 395 nm and 494 nm channels. Conveniently, the 395/494 nm dual-excitation ratio is directly linked to the portion of sensor oxidation; the higher ratio corresponds to stronger GSH oxidation. The compartmental E_{GSH} at steady-state or after treatment with quinones is assigned after probe calibration at the end of the experiment with the chemicals diamide and DTT, which elicit full oxidation and full reduction, respectively.

Under resting conditions both cytosolic (Fig. 1A) and mitochondrial (Fig. 1B) probes expressed in A549 cells are strongly reduced at excitation ratio near 0.1. Following addition of DNQ at a concentration (0.6 μM; t = 1.5 min) that effectively kills cancer cells [8,9], the cytosolic probe showed dramatic change in the 395/494 nm excitation ratio indicating immediate full oxidation within 30 s (Fig. 1A). When treated with a similar DNQ concentration the mGFP2 probe reacted as quickly as the cGFP2 probe, but the increase in oxidation reflected in the 395/495 nm excitation ratio was substantially less (Fig. 1B). Thus, these data demonstrate rapid oxidation in both cytosol and mitochondrial matrix of A549 cells exposed to a NQO1-bioactivated quinone.

To exclude experimental variation and further confirm coordinated compartmental NQO1-bioactivated quinone responses, A549 or MIA-PaCa-2 cell lines stably expressing mGFP2 and cGFP2 were seeded together in the same experimental well and exposed to DNQ. Fig. 1C and D shows fluorescence images of A549 and MIA-PaCa-2 cells with two representative cells selected from each population for data analysis. Below each cell type, corresponding panels display the response of mGFP2 (cells 1, 2) and cGFP2 (cells 3, 4) probes to challenge with DNQ in the absence or presence of NQO1 inhibitor ES936. Because the application of 0.6 μM DNQ elicited a complete oxidative response of cGFP2 in A549 cells (Fig. 1A′), 0.2 μM DNQ was used in further experiments (Fig. 1C, D). This reduced DNQ concentration applied to A549 cells still triggered nearly-full oxidation of the cytosolic probe concomitant with lesser oxidation of the mitochondrial probe (Fig. 1C′). In contrast to A549 cells, similar (0.2 μM) DNQ concentration triggered full mGFP2 oxidation and lesser oxidation of cGFP2 in MIA-PaCa-2 cells (Fig. 1D′). The strong oxidation of the cytosolic probe in A549 cells is consistent with the previously-determined higher NQO1 activity

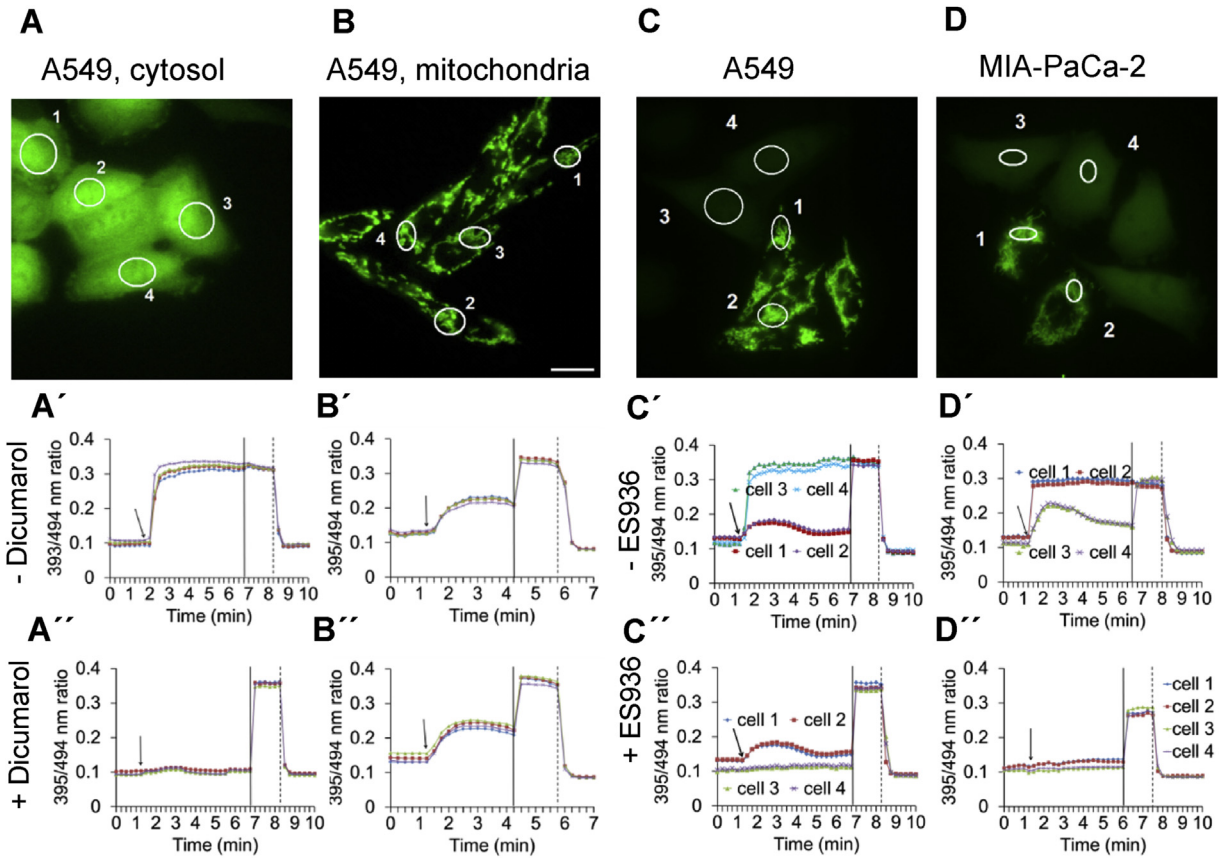

Fig. 1. DNQ-induced cytosolic oxidation is NQO1-dependent, whereas mitochondrial oxidation depends on cell type. Live A549 cell microscopic images showing the expression of Grx1-roGFP2 localized in the (**A**) cytosol (cGFP2) and (**B**) mitochondria (mGFP2) in wells with a single probe and (**C**) A549 and (**D**) MIA-PaCa-2 cell lines with mixed probes (cells 1, 2 with mGFP2 and cells 3, 4 with cGFP2) in a single well. Panels (**A′**–**D′**, **A″**–**D″**) under images are corresponding time-lapse responses of the probe 395/494 nm excitation ratio to treatments with (**A**, **B**) 0.6 μM DNQ (arrow) with or without incubation with 25 μM dicumarol and (**C**, **D**) 0.2 μM DNQ with or without incubation with 0.1 μM ES936 followed by the probe calibration with 2 mM diamide (vertical solid line) and 10 mM dithiothreitol (DTT, vertical dashed line). Scale bar represents 20 μm. Each trace within panels designates a separate cell. The data are representative of three independent experiments with multiple wells using a minimum of four ROIs per well.

level relative to MIA-PaCa-2 cells [9]. Thus, although the quinone's tumor cell killing mechanism relies on cytosolic NQO1-dependent redox cycling consuming oxygen and generating superoxide, DNQ triggers distinct levels of oxidation not only between compartments of a single cell, but also between cell lines. Whereas cytosolic DNQ responses correlate with the previously-established NQO1 enzymatic activity levels determined for A549 and MIA-PaCa-2 cells, mitochondrial responses do not. Therefore, we next asked to what extent NQO1 contributes to these unique responses by monitoring real-time alterations of E_{GSH} in the presence of NQO1 inhibitors.

3.2. NQO1 redox cycling is the main, but not only, determinant of DNQ-induced cellular oxidation

To gain further insight into the mechanism of mitochondrial DNQ response, A549 cells were incubated with dicumarol, a potent inhibitor of NQO1 [24]. The DNQ-induced oxidative response of the cytosolic probe was fully abolished in dicumarol-treated cells as evidenced by an unchanged 395/494 nm excitation ratio near 0.1 both before and after challenge with DNQ (Fig. 1A″), confirming the cytosolic NQO1 enzyme is a major target for DNQ in A549 cells. Interestingly, dicumarol failed to prevent mitochondrial oxidation (Fig. 1B″). This result indicates that DNQ induces oxidation of the mitochondrial matrix compartment independent of NQO1 activity. However, while dicumarol is a competitive inhibitor of NQO1, it has additionally been reported to impair mitochondrial electron transport in human myeloid leukemia cells, and therefore its impact on mitochondrial oxidation cannot be excluded [25]. To account for this possibility, ES936, an alternative irreversible inhibitor of NQO1, was also used. Fig. 1C″ and 1D″ show compartmental responses in A549 and MIA-PaCa-2 cells to challenge with DNQ in the presence of ES936. ES936 effectively abolished DNQ-mediated cytosolic oxidation in both lines whereas the mitochondrial response was distinct between cell lines. Similar to dicumarol, ES936 was ineffective in preventing DNQ-induced mitochondrial oxidation in A549 cells (Fig. 1C″). Hence, mGFP2 oxidation in A549 cells is independent of NQO1 activity and thus represents a marginal off-target effect of DNQ-induced mitochondrial matrix oxidation. In contrast, oxidation in both compartments of MIA-PaCa-2 cells was prevented with ES936 treatment (Fig. 1D″). This result emphasizes that in MIA-PaCa-2 cells NQO1 is the major determinant in DNQ-induced ROS generation leading to tumor-selective killing. Intriguingly, the cytosolic ROS generated via bioreductive activation of DNQ in A549 cells had no significant impact on mGFP2 despite the diffusion of H2O2 from cytosol to mitochondria in A549 cells (not shown). The demonstration that cytosolic and mitochondrial oxidation can be uncoupled from one another and independently elicited as shown in A549 cells may have potential for future manipulations of cellular cytotoxicity

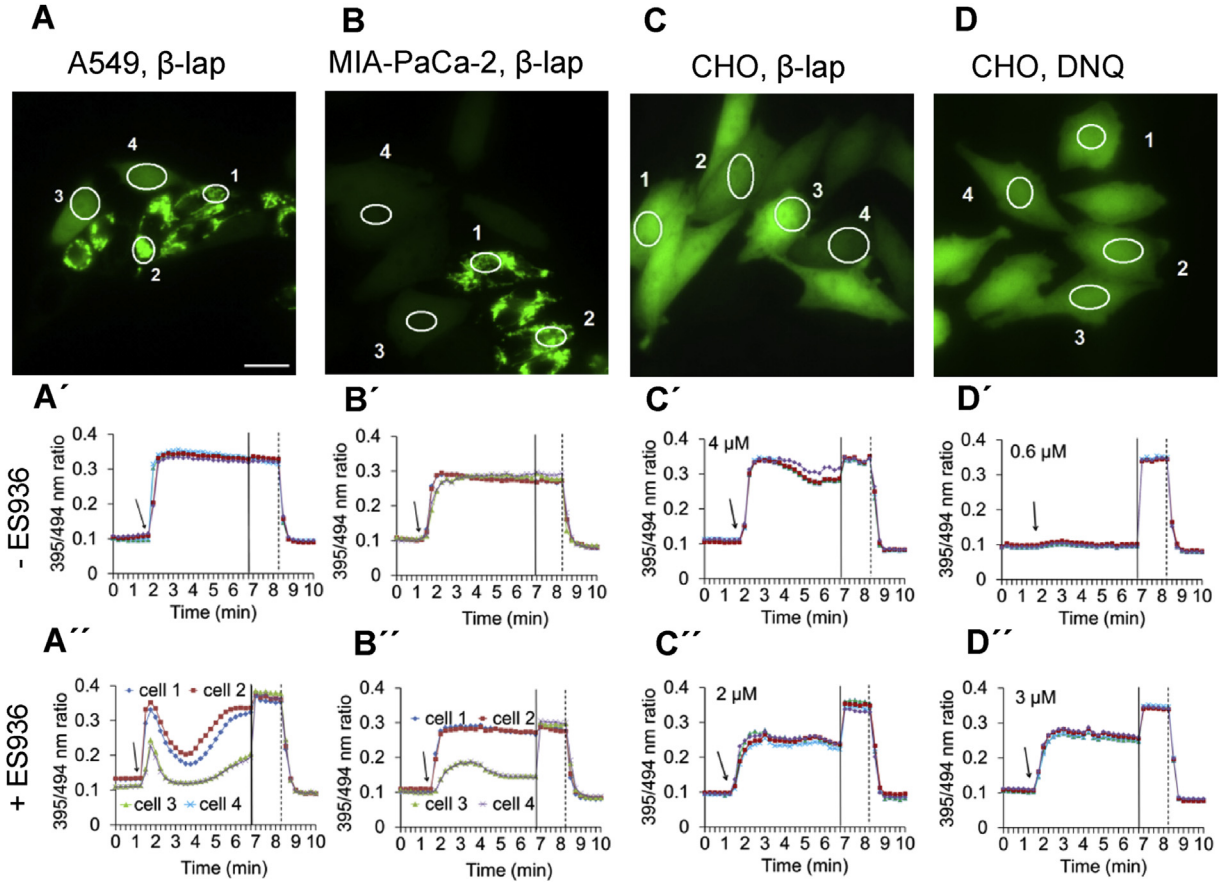

Fig. 2. B-lapachone exhibits direct oxidation of redox-sensitive probe. (**A**) Representative fluorescence images of A549 and (**B**) MIA-PaCa-2 cells showing the expression of Grx1-roGFP2 localized in mitochondria (cells 1 and 2 with mGFP2) and cytosol (cells 3 and 4 with cGFP2). Panels (**A′**, **A″**, **B′**, **B″**) under images are corresponding time-lapse responses of the probe 395/494 nm excitation ratio to treatments with 4 μM β-lap (arrow) with or without 0.2 μM ES936 incubation followed by the probe calibration with 2 mM diamide (vertical solid line) and 10 mM dithiothreitol (DTT, vertical dashed line). (**C**, **D**) Representative fluorescence images of CHO cells showing the expression of Grx1-roGFP2 localized in cytosol. Panels (**C′**, **C″**, **D′**, **D″**) under images are corresponding time-lapse responses of the probe 395/494 nm excitation ratio to treatments with 2 and 4 μM β-lap (arrow) or 0.6 and 3 μM DNQ (arrow) followed by the probe calibration. Scale bar represents 20 μm. Each trace within panels designates a separate cell. The data are representative of three independent experiments.

pathways. Next, oxidative responses to the better characterized chemotherapeutic agent, β–lap, were explored to gain further insight on quinone-induced compartmental ROS generation.

3.3. β-lapachone exhibits NQO1-independent oxidation of redox-sensitive probe

Further biologic characterization of the therapeutic outcome of NQO1-mediated ROS formation is needed for the potent anticancer compound β–lap, which is currently in clinical trials (ARQ-761) [6,26]. Fig. 2A and B show fluorescence images of A549 and MIA-PaCa-2 cells expressing both mGFP2 (cells 1, 2) and cGFP2 (cells 3, 4) probes and their corresponding ratiometric analysis. Differences were not observed between subcellular responses to 4 μM β–lap as both compartments were fully oxidized in all cells (Fig. 2A′, B′). However, the β–lap-induced oxidative responses in presence of ES936 were markedly different from that of DNQ despite sharing a similar mode of action. The concentration of ES936 sufficient to inhibit NQO1 enzymatic activity in MIA-PaCa-2 and A549 could not protect either the cytosolic or mitochondrial matrix probe from β-lap-induced oxidation (Fig. 2A″, 2B″). The oxidation of both probes despite NQO1 inhibition may be interpreted as a reduced reliance on NQO1 for ROS generation; however, this finding would be wholly inconsistent with the previously established mechanism of β-lap-driven ROS generation [2,4].

Another possibility would be a direct impact of β-lap on probe performance. To test that, NQO1-deficient CHO cells were exposed to β-lap treatment [27,28]. Fig. 2C′ shows near full cytosolic oxidation of CHO cells treated with 4 μM β-lap; the level of probe oxidation was substantial when treated with the half maximal inhibitory concentration ($IC_{50} \approx 2$ μM) (Fig. 2C″). In contrast, probe oxidation was not observed in CHO cells exposed to 0.6 μM DNQ which is 10 fold higher than its $IC_{50} \approx 0.06$ μM (Fig. 2D′) in keeping with expectations based upon null NQO1 expression [9]. However, when DNQ was administered in high concentration close to that of β–lap, cytosol oxidation was observed, demonstrating that the compound also has a direct interaction with the probe (Fig. 2D″). Thus, the enhanced NQO1 specificity of DNQ enables lower concentrations to be used *in vivo* and *in vitro*, and allowed further redox investigation without affecting probe performance. Our results are in line with recent evidence of β-lap reduction of cysteines *in vitro* and the suggested alkylation of exposed thiol residues of

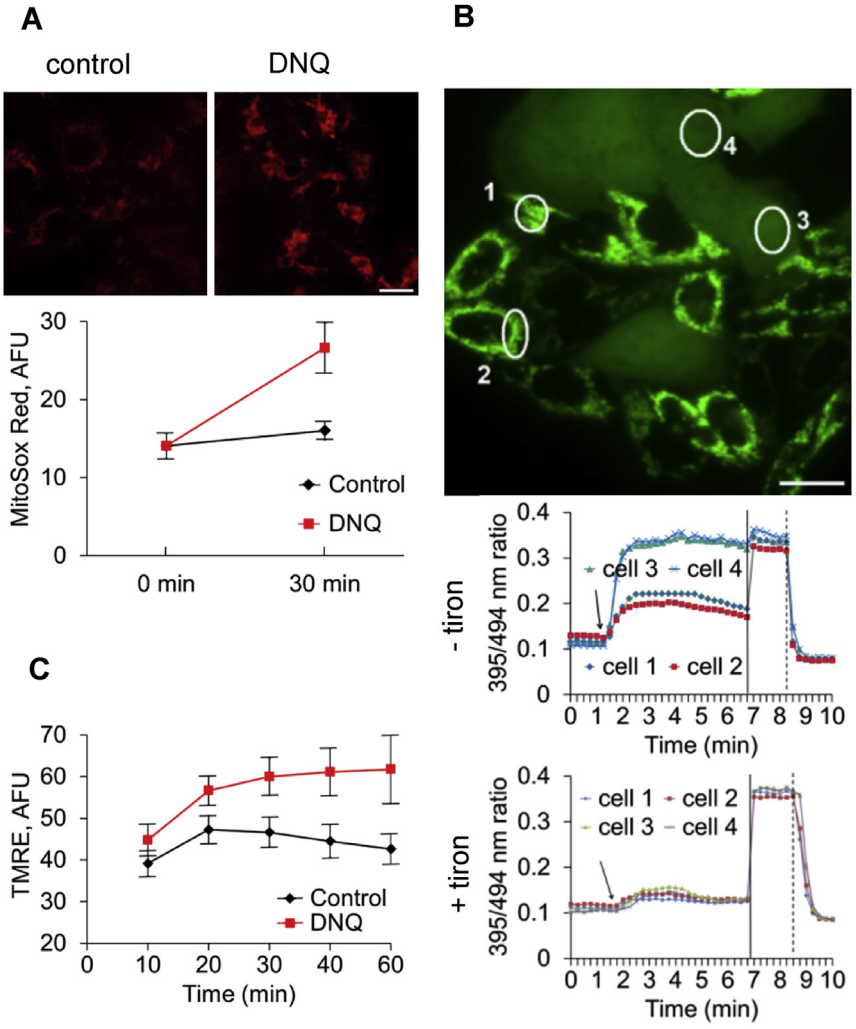

Fig. 3. DNQ induces oxidative responses in mitochondria of A549 cells. (**A**) DNQ increases mitochondrial ROS production and (**C**) induces mitochondrial membrane hyperpolarization. Cells stained with MitoSOX Red (5 μM; **A**) or TMRE (50 nM; **C**) before 0.6 μM DNQ incubation. Fluorescence emission (514 nm excitation) micrographs show changes in ROS with MitoSOX dye after DNQ treatment for 30 min. Plot graphs present corresponding quantitative data at indicated times. The data represent means ± SD (n = 3). DNQ treated cells are statistically different from control $^{*}p < 0.05$. (**B**) Tiron scavenges DNQ-induced ROS in cytosol and mitochondria. Representative fluorescence (Ex 494 nm) image of A549 cells showing Grx1-roGFP2 targeted to the cytosol and mitochondria. Plot graphs are corresponding time-lapse responses of mGFP2 (cells 1, 2) and cGFP2 (cells 3, 4) probes 395/494 nm excitation ratio to treatments with 0.4 μM DNQ of cells with or without incubation with 10 mM tiron for 30 min.

topoisomerase II-DNA complex [29]. Hence, based on the data collected by us and others we hypothesize that both β-lap and DNQ at micromolar concentrations exceeding pharmacologically-relevant levels of DNQ perturb intracellular thiol homeostasis through direct interactions with redox-sensitive cysteines. This β-lap off-target effect may underlie undesirable side effects, as both normal and tumor cells would be affected. Thus, DNQ may be considered as a novel anticancer drug candidate alternative to β-lap for solid tumors with reduced damage to normal cells.

3.4. DNQ triggers mitochondrial ROS production and an initial increase in membrane potential

To further study A549 cell NQO1-independent mitochondrial response to DNQ, fluorescent dyes MitoSOX Red and TMRE were used to examine corresponding changes in mitochondrial ROS production and mitochondrial membrane potential ($\Delta\Psi m$), respectively (Fig. 3A, C). Quantitative analysis of DNQ-treated A549 cells revealed significant (2 fold) increase in MitoSOX fluorescence intensity compared to untreated control cells, confirming the observed oxidation of the mito-Grx1-roGFP2 probe (Fig. 3A). In keeping with NQO1-based ROS generation, treatment with the membrane-permeable ROS scavenger 4,5-dihydroxy-1,3-benzenedisulfonic acid (tiron) neutralized DNQ-driven oxidation of both mGFP2 and cGFP2 probes compared with tiron-free cells (Fig. 3B). A549 cells also responded to DNQ by an immediate increase in $\Delta\Psi m$ as evidenced by relative changes in TMRE fluorescence (Fig. 3C). Collectively these data indicate that by inducing ROS production, oxidizing glutathione, and altering mitochondrial membrane potential, DNQ treatment alters mitochondrial redox homeostasis.

The present study aimed to characterize responses of compartmentalized glutathione redox potentials induced by the pharmacologic quinones DNQ and β-lap. While cytosolic NQO1 is the natural cellular target of these quinones, oxidation of the redox probe was observed in the mitochondrial matrix of A549 cells even following complete NQO1 inhibition. This oxidation was confirmed by measureable mitochondrial ROS release and linked to increased MMP, indications that prolonged exposure may lead to mitochondrial-induced apoptosis. Further, with treatment of pharmacological concentrations of β-lap, both DNQ and β-lap exerted undesired oxidative effects on intracellular thiols; however, the enhanced specificity of DNQ for NQO1 mediates use of concentrations well below this threshold, thereby reducing risk for off-target effects during chemotherapeutic intervention.

Ethical approval

Compliance with ethical standards.

Conflict of interest

The authors declare no conflict of interest.

Acknowledgments

We thank Professor Paul Hergenrother and Dr. Elizabeth Parkinson, Department of Chemistry and Dr. Mayandi Sivaguru of the Carl R. Woese Institute for Genomic Biology for their assistance. This work was supported by National Institutes of Health (NIH) Grant: R33-CA137719 (HR Gaskins & PJ Kenis).

References

[1] G.T. Wondrak, Redox-directed cancer therapeutics: molecular mechanisms and opportunities, Antioxid. Redox Signal 11 (2009) 3013–3069.
[2] J.J. Pink, S.M. Planchon, C. Tagliarino, et al., NAD(P)H: quinone oxidoreductase activity is the principal determinant of beta-lapachone cytotoxicity, J. Biol. Chem. 275 (2000) 5416–5424.
[3] D. Siegel, C. Yan, D. Ross, NAD(P)H:quinone oxidoreductase 1 (NQO1) in the sensitivity and resistance to antitumor quinones, Biochem. Pharmacol. 83 (2012) 1033–1040.
[4] E.A. Bey, M.S. Bentle, K.E. Reinicke, et al., An NQO1- and PARP-1-mediated cell death pathway induced in non-small-cell lung cancer cells by beta-lapachone, Proc. Natl. Acad. Sci. U. S. A. 104 (2007) 11832–11837.
[5] Y. Dong, E.A. Bey, L.S. Li, et al., Prostate cancer radiosensitization through poly(ADP-Ribose) polymerase-1 hyperactivation, Cancer Res. 70 (2010) 8088–8096.
[6] G. Chakrabarti, M.A. Silvers, M. Ilcheva, et al., Tumor-selective use of DNA base excision repair inhibition in pancreatic cancer using the NQO1 bioactivatable drug, beta-lapachone, Sci. Rep. 5 (2015) 17066.
[7] J.S. Bair, R. Palchaudhuri, P.J. Hergenrother, Chemistry and biology of deoxynyboquinone, a potent inducer of cancer cell death, J. Am. Chem. Soc. 132 (2010) 5469–5478.
[8] X. Huang, Y. Dong, E.A. Bey, et al., An NQO1 substrate with potent antitumor activity that selectively kills by PARP1-induced programmed necrosis, Cancer Res. 72 (2012) 3038–3047.
[9] E.I. Parkinson, J.S. Bair, M. Cismesia, P.J. Hergenrother, Efficient NQO1 substrates are potent and selective anticancer agents, J. Am. Chem. Soc. 8 (2013) 2173–2183.
[10] J.Z. Li, Y. Ke, H.P. Misra, et al., Mechanistic studies of cancer cell mitochondria- and NQO1-mediated redox activation of beta-lapachone, a potentially novel anticancer agent, Toxicol. Appl. Pharmacol. 281 (2014) 285–293.
[11] M. Menacho-Marquez, C.J. Rodriguez-Hernandez, M.A. Villaronga, et al., eIF2 kinases mediate beta-lapachone toxicity in yeast and human cancer cells, Cell Cycle 14 (2015) 630–640.
[12] Z. Moore, G. Chakrabarti, X. Luo, et al., NAMPT inhibition sensitizes pancreatic adenocarcinoma cells to tumor-selective, PAR-independent metabolic catastrophe and cell death induced by beta-lapachone, Cell Death Dis. 6 (2015) e1599.
[13] T. He, A. Banach-Latapy, L. Vernis, et al., Peroxiredoxin 1 knockdown potentiates beta-lapachone cytotoxicity through modulation of reactive oxygen species and mitogen-activated protein kinase signals, Carcinogenesis 34 (2013) 760–769.
[14] E.A. Bey, K.E. Reinicke, M.C. Srougi, et al., Catalase abrogates beta-lapachone-induced PARP1 hyperactivation-directed programmed necrosis in NQO1-positive breast cancers, Mol. Cancer Ther. 12 (2013) 2110–2120.
[15] N. Ponnuraj, V.L. Kolossov, E. Parkinson, A. Benefiel, P. Hergenrother, H.R. Gaskins, Deoxynyboquinone and its derivatives upregulate glutathione-specific genes in MDA-MB-231 breast cancer cells, FASEB J. 28 (2014). S 655.610.
[16] F.Q. Schafer, G.R. Buettner, Redox environment of the cell as viewed through the redox state of the glutathione disulfide/glutathione couple, Free Radic. Biol. Med. 30 (2001) 1191–1212.
[17] Y.M. Go, D.P. Jones, Redox compartmentalization in eukaryotic cells, Biochim. Biophys. Acta 1780 (2008) 1273–1290.
[18] M. Gutscher, A.L. Pauleau, L. Marty, et al., Real-time imaging of the intracellular glutathione redox potential, Nat. Met. 5 (2008) 553–559.
[19] M. Schwarzlander, T.P. Dick, A.J. Meyer, B. Morgan, Dissecting redox biology using fluorescent protein sensors, Antioxid. Redox Signal 24 (2016) 680–712.
[20] V.L. Kolossov, W.P. Hanafin, J.N. Beaudoin, et al., Featured Article: inhibition of glutathione synthesis distinctly alters mitochondrial and cytosolic redox poise, Exp. Biol. Med. Maywood 239 (2014) 394–403.
[21] V.L. Kolossov, B.Q. Spring, A. Sokolowski, et al., Engineering redox-sensitive linkers for genetically encoded FRET-based biosensors, Exp. Biol. Med. 233 (2008) 238–248.
[22] V.L. Kolossov, J.N. Beaudoin, N. Prabhu Ponnuraj, et al., Thiol-based antioxidants elicit mitochondrial oxidation via respiratory complex III, Am. J. Physiol. Cell Physiol. 309 (2015) C81–C91.
[23] M.S. Bentle, K.E. Reinicke, E.A. Bey, et al., Calcium-dependent modulation of poly(ADP-ribose) polymerase-1 alters cellular metabolism and DNA repair, J. Biol. Chem. 281 (2006) 33684–33696.
[24] P.C. Preusch, D. Siegel, N.W. Gibson, D. Ross, A note on the inhibition of DT-diaphorase by dicoumarol, Free Radic. Biol. Med. 11 (1991) 77–80.
[25] D. Gonzalez-Aragon, J. Ariza, J.M. Villalba, Dicoumarol impairs mitochondrial electron transport and pyrimidine biosynthesis in human myeloid leukemia HL-60 cells, Biochem. Pharmacol. 73 (2007) 427–439.
[26] A.Y. Gerber, M.S. Beg, J.E. Dowell, J.H. Schiller, A.E. Frankel, et al., Phase 1 correlative study of ARQ761, a b-lapachone analogue that promotes NQ01-mediated programmed cancer cell necrosis, Eur. J. Cancer 50 (2014) 84–85.
[27] A.S. Tan, M.V. Berridge, Evidence for NAD(P)H:quinone oxidoreductase 1 (NQO1)-mediated quinone-dependent redox cycling via plasma membrane electron transport: a sensitive cellular assay for NQO1, Free Radic. Biol. Med.

48 (2010) 421–429.
[28] L.H. De Haan, A.M. Boerboom, I.M. Rietjens, et al., A physiological threshold for protection against menadione toxicity by human NAD(P)H:quinone oxidoreductase (NQO1) in Chinese hamster ovary (CHO) cells, Biochem. Pharmacol. 64 (2002) 1597–1603.
[29] A.M. Oliveira-Brett, M.O. Goulart, F.C. Abreu, Reduction of lapachones and their reaction with L-cysteine and mercaptoethanol on glassy carbon electrodes, Bioelectrochemistry 56 (2002) 53–55.